frontiers | Frontiers in Marine Science

TYPE Original Research
PUBLISHED 06 November 2024
DOI 10.3389/fmars.2024.1423721

OPEN ACCESS

EDITED BY
Sid Knotek,
Faculty of Veterinary Medicine, Czechia

REVIEWED BY
Javier Nevarez,
Louisiana State University, United States
Michaela Gumpenberger,
University of Veterinary Medicine Vienna, Austria

*CORRESPONDENCE
Brian Chin Wing Kot
briankot@cityu.edu.hk;
briankot@yahoo.co.uk

RECEIVED 26 April 2024
ACCEPTED 16 September 2024
PUBLISHED 06 November 2024

CITATION
Yeong WY, Martelli P, Chung TYT, Tsui HCL, Gerussi T and Kot BCW (2024) Ultrasonographic technique and appearance of the coelomic organs in crocodilians. *Front. Mar. Sci.* 11:1423721. doi: 10.3389/fmars.2024.1423721

Ultrasonographic technique and appearance of the coelomic organs in crocodilians

Wei Yeng Yeong[1,2], Paolo Martelli[3], Tabris Yik To Chung[2], Henry Chun Lok Tsui[2], Tommaso Gerussi[2] and Brian Chin Wing Kot[2,4]*

[1]Jockey Club College of Veterinary Medicine and Life Sciences, City University of Hong Kong, Hong Kong, Hong Kong SAR, China, [2]Department of Infectious Diseases and Public Health, Jockey Club College of Veterinary Medicine and Life Sciences, City University of Hong Kong, Hong Kong, Hong Kong SAR, China, [3]Veterinary Hospital, Zoological Operations and Conservation, Ocean Park Corporation, Hong Kong, Hong Kong SAR, China, [4]Department of Chemistry, College of Science, City University of Hong Kong, Hong Kong, Hong Kong SAR, China

Introduction: Crocodilians have significant ecological, conservational, and economic roles. They are also commonly raised for commercial purposes and kept as zoological specimens. Although ultrasonography has been used in zoological contexts for health assessments of crocodilians, published studies on a detailed ultrasonography protocol and ultrasonographic anatomy are lacking. This study aimed to establish a standardized ultrasonography protocol and pictorial reference of the ultrasonographic appearances of the coelomic organs of crocodilians.

Methods: A total of 7 crocodilians comprising 4 different species were included in this study. The crocodilians were manually restrained and underwent a non-contrasted and contrasted computed tomography (CT) scan, followed by an ultrasonography (USG) examination. Ultrasound fusion imaging technique enabled greater confidence in establishing a clear organ localization and correlation between modalities by visualizing the same anatomy from the same view angle.

Results: The heart, caudal vena cava, liver, fat body (steatotheca), spleen, stomach, duodenal loops, pancreas, kidneys, testes, ovaries and cloaca were visualized in all species. Longitudinal and transverse images of the coelomic structures were acquired when possible. The ultrasonographic characteristics of the coelomic organs, including transducer positioning, acoustic window and approach, shape, size, marginations, and echo pattern were documented.

Discussion: The findings of this study provided a useful ultrasonographic protocol and anatomical reference of the coelomic organs in crocodilians. Invaluable insights into the practicality and adequacy of ultrasonography in evaluating the coelomic structures of crocodilians as part of health assessment and disease diagnosis were also discussed.

KEYWORDS

ultrasonography, crocodile, reptile, coelom, imaging anatomy, fusion imaging, computed tomography

1 Introduction

According to the taxonomy accepted by the International Union for the Conservation for Nature (IUCN), there are 26 species of crocodilians under the order *Crocodilia* subdivided into 3 families (*Alligatoridae* – alligators and caimans, *Crocodylidae* – true crocodiles, and *Gavialidae* – gharials and false gharials) and 9 genera (IUCN Crocodile Specialist Group, 2022a). In the wild, crocodilians are apex predatory reptiles that inhabit tropical and subtropical wetlands globally (Huchzermeyer, 2003). They are keystone species that maintain ecosystem structure and function through various activities, including selective predation of prey species, physical alteration of the environment, and nutrient recycling (Nifong, 2018). In the late 19th century, rapid population depletion of wild crocodilians occurred due to over-hunting and destruction of natural habitats by anthropogenic activities including deforestation, pollution, and conversion of land to agricultural use (Ross, 1998). With the establishment of the IUCN Crocodilian Specialist Group (CSG) in the 1970s, various conservational interventions have been implemented, including ranching i.e., obtaining a wild source of eggs and young to rear in captivity and farming i.e., keeping breeding stock on a farm and producing their own source of young (Brazaitis and Watkins-Colwell, 2011). While several species have recovered or are recovering, 7 species are currently still 'critically endangered' and 4 species are 'vulnerable' under the IUCN Red List of Threatened Species. The Convention on International Trade in Endangered Species of Wild Fauna and Flora (CITES) has listed all living crocodilian species in Appendix I and II to minimize the threats to their survival related to international trading (Brazaitis and Watkins-Colwell, 2011).

In crocodilian farms, veterinary management is crucial to minimize disease-related production losses (Lovely et al., 2007). Health assessments are also valuable to ensure individuals are well-nourished and are free of crocodilian-specific infectious agents prior to conservation releases into the wild (Huchzermeyer, 2003). However, the current practice of health assessments via visual, physical, clinical, hematological and biochemical examinations has its limitations. Firstly, crocodilians rarely display clinical signs in the early stages of diseases. The presence of osteoderms and gastralia restricts the feasibility of palpating internal organs (Huchzermeyer, 2003). A normal reference range for hematology and serum biochemistry is still lacking for many species and there are notable inter- and intraspecies variations and effects of environmental conditions, e.g., the seasonal period and diet, limit their applicability across populations (Huchzermeyer, 2003; Peng et al., 2018; Latip et al., 2021). Intracelomic diseases often remain unidentified without performing a necropsy (Nevarez, 2019). Although ultrasonography (USG) has been applied in zoological settings for health assessments of crocodilians, there is scarce literature available on USG protocol and ultrasonographic anatomy for crocodilians. At present, only an overview of the general applications of USG in crocodilians (Martelli, 2019) and two descriptions for assessing the reproductive status (Tucker and Limpus, 1997; Lance et al., 2009) of crocodilians using USG have been published.

A standardized protocol can contribute to a more comprehensive and systematic health assessment of crocodilians under human care, optimizing animal handling time for imaging and increasing the validity of imaging examinations (McDougald et al., 2020). A well-documented diagnostic imaging reference of the normal ultrasonographic appearance of crocodilians will be a valuable guide for field researchers, veterinarians, and aquarium staff in acquiring and interpreting diagnostic images and aiding corrective interventions. Therefore, this research paper aims to establish a ultrasonographic protocol and provide pictorial references on the normal ultrasonographic anatomy of coelomic organs in crocodilians.

2 Materials and methods

This was a cross-sectional prospective study conducted from November 2022 to April 2023 in Hong Kong, SAR. All 7 captive crocodilians (of 4 different species) residing in 3 different conservation institutions in Hong Kong were recruited as the study subjects: 3 Chinese alligators (*Alligator sinensis;* 1 male and 2 females), 1 spectacled caiman (*Caiman crocodilus*; female), 1 saltwater crocodile (*Crocodylus porosus*; female) and 2 false gharials (*Tomistoma schlegelli;* 1 male and 1 female). The crocodilian species, residing institutes, sex, weight and head-tail length were listed in Table 1. All animals were in apparent fine health, based on clinical history, complete physical examination and comparison of hematology and serum biochemistry results with previous routine self-reference parameters. All clinical examinations were performed by a veterinarian with 25+ years of experience in crocodilian conservation, board-certified by the Asian College for Conservation Medicine and chair of the veterinary Science group of the IUCN Crocodilian Specialist Group. All crocodilians were kept in outdoor enclosures and were not fasted for the study. Ethical approval for this study was obtained from the Animal Research Ethics Sub-Committee, City University of Hong Kong and the 3 conservation institutes. A license under the Animals (Control of Experiments) Ordinance (Cap. 340) from the Department of Health, Hong Kong was also acquired to conduct this study.

2.1 Animal restraining and transportation

Only one animal was examined in each session to prevent unnecessary handling stress of other crocodilians. A team of 5-10 trained individuals were involved in each restraining process depending on the size of the crocodile. The animals were manually restrained in their respective enclosures and transported to Ocean Park Hong Kong for the CT and USG examinations. The immobilization protocol was led by the same veterinarian (PM) with reference to the Crocodilian Capacity Building Manual (IUCN Crocodile Specialist Group, 2022b). In general, the subjects were immobilized by tying their limbs to a frame, and their snouts with cotton ropes and eyes with a towel to keep them calm (Figure 1). Chemical restraint was not used in the study. The crocodilians were transported back to their respective enclosures immediately after the imaging examinations.

TABLE 1 Information on the study subjects including the crocodilian species, respective institutes, sex, weight and length.

Study subject species	Conservation institute	Sex	Weight (kg)	Head-tail length (cm)
Chinese alligator (*Alligator sinensis)*	OPHK	M	27.0	156
Chinese alligator (*Alligator sinensis)*	OPHK	F	19.0	160
Chinese alligator (*Alligator sinensis)*	KFBG	F	18.0	160
Spectacled caiman (*Caiman crocodilus)*	KFBG	F	26.7	140
False gharial (*Tomistoma schlegelii)*	HKWP	M	130.0	299
False gharial (*Tomistoma schlegelii)*	HKWP	F	88.6	276
Saltwater crocodile (*Crocodylus porosus*)	HKWP	F	118.2	297

OPHK, Ocean Park Hong Kong; KFBG, Kadoorie Farm and Botanical Garden; HKWP, Hong Kong Wetland Park; M, male; F, female.

2.2 Computed tomography

All animals underwent a plain and contrast-enhanced CT scan focusing on the coelomic cavity, prior to the USG examination to provide an initial topographic assessment of the coelomic structures for more accurate organ detection and correlation with ultrasonographic findings. All animals were manually restrained in sternal recumbency on the CT couch in a craniocaudal direction towards the CT gantry. The animals were secured with cotton ropes onto a bamboo ladder topped with a styrofoam cushion to minimize positional anatomical disruptions. A Philips 16-slice Brilliance Big Bore CT scanner (Philips Healthcare, Amsterdam, Netherlands) was used with the following exposure parameters: 100–140 kV, 101–343 mA, 0.8-1.6 mm slice thickness, and scan field of view of 406–600 mm. Exposure parameters were adjusted according to subject size to optimize image quality. After a plain CT scan was obtained, an intravenous iodinated contrast medium (Visipaque 270mg/ml; GE Healthcare Inc., Marlborough, MA, U.S.A) was injected by the veterinarian (PM) into the occipital venous sinus at a dose of 2 mL/kg for a contrast-enhanced CT scan. All CT datasets were reconstructed and reported via the TeraRecon Aquarius iNtuition workstation (TeraTecon Inc., San Mateo, CA, USA) (Kot et al., 2016, 2020a) by a board-certified diagnostic imaging clinician with 20+ years of experience in aquatic animal diagnostic imaging and imaging anatomy (BCWK).

2.3 Fusion imaging technique

A fusion imaging technique synchronizing CT imaging datasets with real-time USG was incorporated into the study to enable greater confidence in establishing a clear organ localization and correlation between modalities by visualizing the same anatomy from the same view angle. Prior to the CT scan, 7 external CT markers were placed on different areas of the skin of the coelomic region dorsally and laterally as landmarks for fusion with the USG examination. After the CT scans were obtained, the CT dataset was loaded onto a MyLab™ Twice ultrasound unit (Esaote SpA, Genoa,

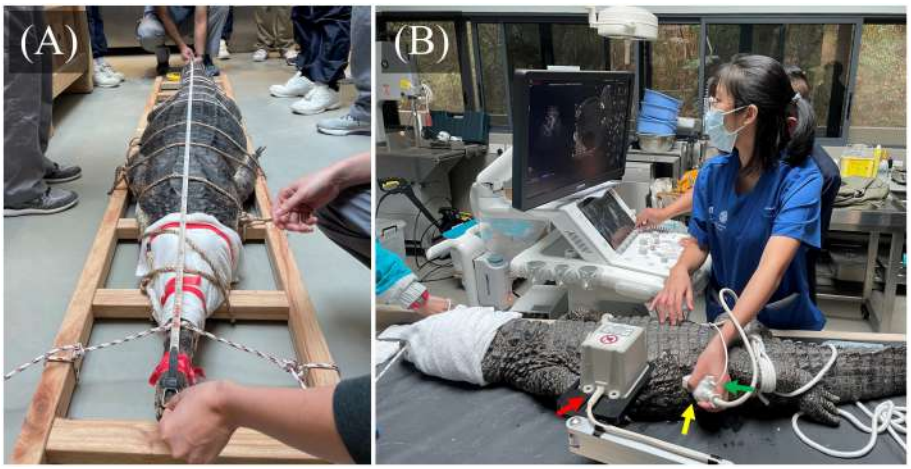

FIGURE 1
Examples of restrain of animals in the study. **(A)** A 90kg false gharial was immobilized by tying it to a frame using ropes and securing its head and jaws with towels and tapes. **(B)** A 20kg Chinese alligator was restrained with ropes and positioned in sternal recumbency for the USG procedure. The USG (with fusion imaging capacity) machine was set up with the electromagnetic tracking device (red arrow) placed near the subject. A curvilinear probe (yellow arrow) with a magnetic position sensor (green arrow) attached to it was used. The synchronized CT images and real-time ultrasound windows were displayed simultaneously on the USG screen.

Italy). A magnetic positioning sensor was placed within 1-meter proximity to the crocodilian for synchronization (Pang et al., 2006; Kot et al., 2009). Using Esaote's Virtual Navigator and Fusion Imaging software, the coelomic organs were assessed with real-time USG while correlating with the reconstructed CT images.

2.4 Ultrasonography

Ultrasonography examination was performed immediately after the CT scans by a final year veterinary medicine student under the supervision training of a board-certified diagnostic radiographer imaging clinician (BCWK) and a wildlife veterinarian (PM). Real-time B mode ultrasound examinations were conducted using MyLab™ Delta (Esaote SpA, Genoa, Italy) or MyLab™ Twice (Esaote SpA, Genoa, Italy) ultrasound units, in conjunction with a 2-5 MHz curvilinear transducer. The color Doppler technique was used to assess organ vasculature. Ultrasound gel was copiously applied onto the area of contact on the skin immediately prior to the examination to dampen and fill in the irregularities of the skin. Each coelomic organ was thoroughly assessed longitudinally and transversely, and corresponding sonograms and video clips were obtained. The ultrasonographic characteristics including transducer positioning, acoustic window and approach, shape, size, marginations and echo pattern were documented. All ultrasound protocols were made by the consensus of all authors. The ultrasound examination lasted 20 minutes for each animal. After the procedures, the CT and ultrasound images were reviewed simultaneously and compared with unpublished necropsy images of Siamese and estuarine crocodiles from PM to confirm the topographic coelomic organ anatomy and their corresponding ultrasonographic findings.

3 Results

3.1 Computed tomography protocol

The CT scans were carried out smoothly with no side effects from mechanical restraint and CT contrast injection via the occipital venous sinus. The post-contrast time, determined by the washout of contrast medium from kidneys, ranged between 8 to 10 minutes to obtain images of the coelomic organs with adequate contrast perfusion (Figure 2). The quality of the reconstructed CT images was consistent between different species.

3.2 Ultrasonography protocol

The use of various acoustic windows, transducer positioning and orientations (Figure 3) allowed the visualisation of the heart, liver, caudal vena cava, gallbladder, spleen, fat body (steatotheca), stomach, duodenal loops, pancreas, follicles, testes, kidneys, and cloaca. Fanning and compression techniques were used to assess larger structures, including the liver, fat body, stomach and ovarian follicles.

The crocodilians were first examined in sternal recumbency and then turned over to be examined in dorsal recumbency. On sternal recumbency, the intercostal space allowed for proper examination of the liver and pleura surface of the lungs. From the left lateral

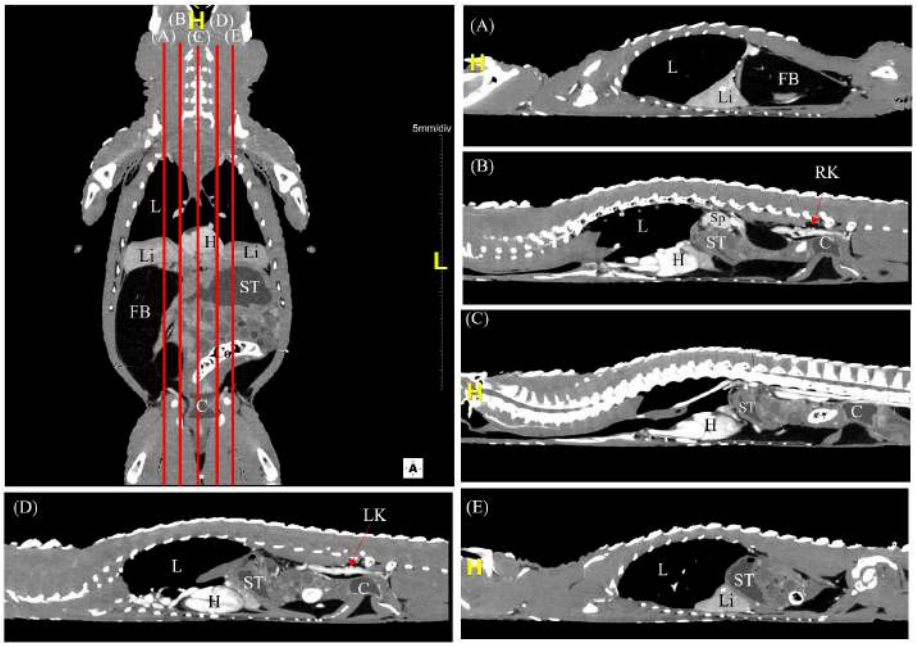

FIGURE 2
A labelled coronal contrast-enhanced CT image of an *Alligator sinensis* with corresponding parasagittal **(A, B, D, E)** and mid-sagittal **(C)** views in soft tissue window. [Highlighted in yellow, H, head/cranial; L, left; C, cloaca; Co, colon; FB, fat body; H, heart; L, lung; Li, liver; LK, left kidney; RK, right kidney; ST, stomach; Sp, spleen].

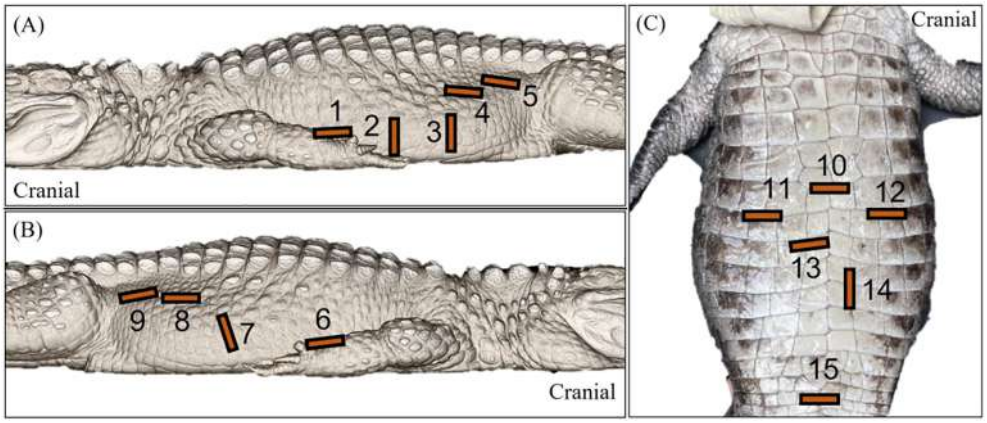

FIGURE 3
Labelled images of an *Alligator sinensis* to depict the general transducer positioning 1 to 15 via the **(A)** left lateral, **(B)** right lateral and **(C)** ventral approaches. [1=sagittal view of the left liver lobe and the heart; 2=transverse view of the stomach 3=transverse view of the ovarian follicles in active female crocodilians and the intestines; 4=sagittal view of the testes; 5=sagittal view of the left kidney; 6= sagittal view of the right liver lobe, intrahepatic caudal vena cava and the heart; 7=transverse view of the fat body, spleen and gallbladder and sagittal view of the duodenal loops; 8=sagittal view of the testes; 9=sagittal view of the right kidney; 10=transverse view of the heart; 11=transverse view of the right liver lobe; 12=transverse view of the left liver lobe; 13=transverse view of the gallbladder; 14=transverse view of the duodenal loops; 15=transverse view of the cloaca].

approach, the left liver lobe, stomach, duodenal loops, pancreas, follicles, left testes, and left kidney were visualised. The right liver lobe, gall bladder, fat body and spleen were best visualised from the right lateral approach. On dorsal recumbency, the transducer had to be placed in between the ventral scutes to avoid interference by the osteoderms. The ventral aspect allowed a better assessment of the heart than the lateral trunk. However, due to the difference in ventral osteoderm coverage of different species, the ventral side was a poor acoustic window for the spectacled caiman and false gharials but allowed proper assessment of the heart, liver, gallbladder, stomach, duodenal loops and cloaca for the Chinese alligators and the saltwater crocodile. The cloaca was examinable ventrodorsally when distended via the pelvic inlet without being affected by the osteoderms.

3.3 Ultrasonographic anatomy

3.3.1 Heart

The 4-chambered heart of the crocodilians was located medioventrally in the cranial coelom and almost entirely encircled by the left and right liver lobes (Figures 2, 4). The heart could be visualized in 7/7 animals laterally in between the intercostal spaces, but the examination was poor due to its deep position in the center of the coelom and hindrance by the acoustic shadows from the ribs. The heart was best visualized with the animal placed on its back and the transducer placed at the ventral midline one-third to midway between the axilla to the vent (Figure 2, transducer position 10). The 4 heart chambers (2 atria and 2 ventricles) and cardiac contractions were clearly visualized in the Chinese alligators and the saltwater crocodile. Both transverse and longitudinal images of the heart were obtained (Figures 5A, B). In the caiman and false gharials, the heart was poorly visualized ventrally due to the large and dense osteoderms of the ventral scales which hindered the ultrasound beam propagation into the coelomic organs. The myocardium was homogenous and isoechoic to the adjacent liver. Blood in the heart chambers was anechoic. The ventricles had thicker muscular walls compared to the atria. In sagittal orientation, the muscular ventricular septum was identified between the left and right ventricles. Pericardial fluid was easily visualized in the pericardium for all animals.

3.3.2 Liver

The liver was visualized in 7/7 animals and could be entirely scanned. The left and right liver lobes, of similar size, were wedged caudally with tapered ends and craniodorsally bordered by the lungs, caudally by the stomach on the left and fat body on the right, and medially by the heart (Figures 2, 4). Transducer placement in the 5^{th} to 7^{th} intercostal space on the lateral trunks allowed visualization of the liver lobes (Figure 3, transducer positions 1 and 6). Placement of the probe between the ventral scales transversely adjacent to the level of the heart also allowed visualization of the triangular cross-section of the liver lobes (Figure 3, transducer position 11 and 12; Figure 6B). The liver lobes were encapsulated with a hyperechoic rim. The hepatic parenchyma was homogenous and highly vascularized. It was isoechoic to the stomach wall and more hyperechoic than the fat body (except in the Caiman the fat body was more hyperechoic). From the right side, the intrahepatic caudal vena cava was seen exiting the right liver lobe into the right atrium in a craniomedial fashion (Figure 6A). It was the largest vessel with an echogenic wall and an anechoic lumen coursing the hepatic parenchyma. The hepatic veins with echogenic walls branching off the caudal vena cava were also visualized. However, other hepatic vessels, including the portal vessels, were not often discernible based on ultrasonographic appearance.

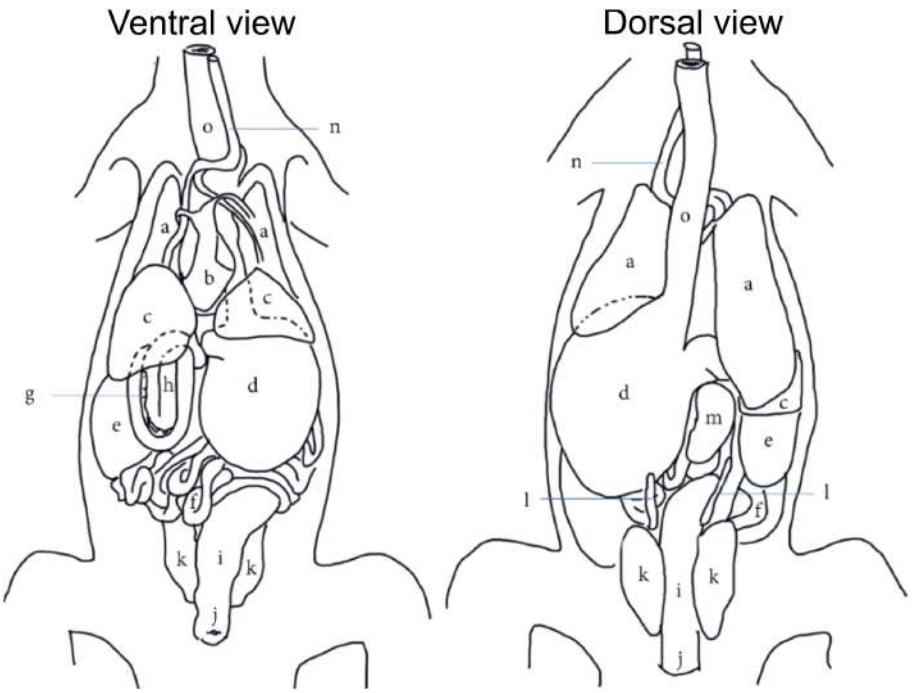

FIGURE 4
A generic topographical anatomy of the coelomic organs of crocodilians in ventral and dorsal views adapted and modified from Van Der Merwe and Kotze (1993). [a=lungs; b=heart; c=liver; d=stomach; e=fat body; f=jejunal and ileal loops; g=pancreas; h=duodenal loops; i,=colorectum; j=cloaca; k=kidneys; l=gonads; m=spleen; n=trachea; o=esophagus].

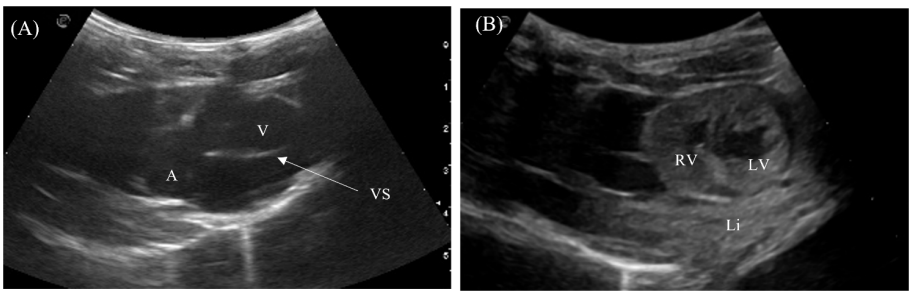

FIGURE 5
Ultrasonographic appearance of the heart in **(A)** sagittal and **(B)** transverse views from the ventral approach in *Alligator sinensis*. [Li, liver; RV, right ventricle; LV, left ventricle; VS, ventricular septum].

3.3.3 Gallbladder

The gallbladder was a fluid-filled sac located ventromedially caudal to the right liver lobe. It was visualized in 6/7 of the crocodilians except for the saltwater crocodile. The transducer was placed on the mid-portion of the right flank and directed ventrally, using the fat body as an acoustic window (Figure 3, transducer position 7). It was also visible ventrally if not obstructed by the osteoderms (Figure 3, transducer position 13). The gallbladder was visualized as an irregular globular structure with a thin hyperechoic wall filled with hypoechoic to anechoic content (Figure 7).

3.3.4 Fat body (steatotheca)

The fat body was a clearly visualized organ in 7/7 animals orienting craniocaudally in the right coelom (Figure 2). It varied in size with body condition and could be as large as a liver lobe or smaller than the spleen. The fat body was heterogenous with coarse echotexture and small, diffuse hyperechoic foci and lines. It was hypoechoic relative to the liver and well-encapsulated with a smooth and regular hyperechoic rim (Figure 8A). Hyperechoic hila parallel to the transducer were visualized, and vascularity was detected using Doppler ultrasound (Figure 8B). In the Chinese alligators, the fat body extended caudally over to the left coelom, which could be visualized from the caudal left flank.

3.3.5 Spleen

The spleen was an ovoid organ positioned mediodorsally in the mid-coelom caudal to the liver lobes (Figure 4). It was visualized in 7/7 crocodilians with the transducer placed on the mid-right flank

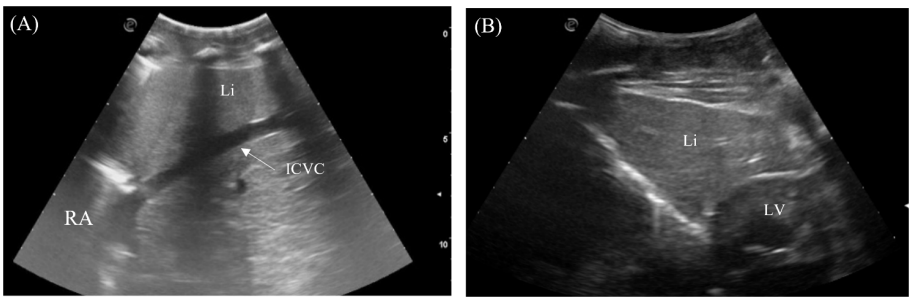

FIGURE 6
Ultrasonographic appearance of the **(A)** right liver lobe with intrahepatic caudal vena cava from the right lateral view in *Caiman crocodilus* and **(B)** the left liver lobe from the ventral view in *Alligator sinensis*. [ICVC, intrahepatic caudal vena cava; LLi, left liver lobe; LV, left ventricle; RA, Right atrium; Rli, right liver lobe].

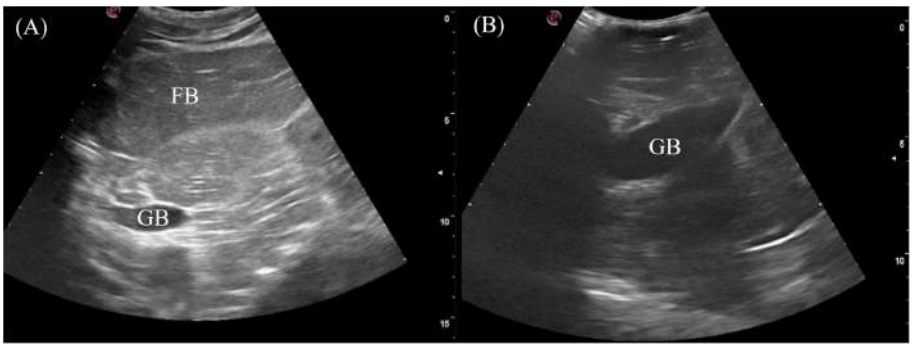

FIGURE 7
Ultrasonographic appearance of the gallbladder in sagittal via the **(A)** right lateral view in *Alligator sinensis* and **(B)** the ventral view in *Tomistoma schlegelii*. [FB, fat body; GB, gallbladder].

and directed dorsally (Figure 3, transducer position 7). The spleen was well-marginated with a thin, hyperechoic border. The parenchyma was homogenous and more hyperechoic than the adjacent fat body (Figure 9).

3.3.6 Gastrointestinal tract and pancreas

The stomach was immediately adjacent to the left coelomic wall caudal to the left liver lobe. The gastric fundus was visualized in 7/7 animals from the left lateral view intercostally and just caudal to the last rib (Figure 3, transducer position 2). The entire gastric fundic wall could be visualized with the transducer when filled with anechoic fluid. Small amounts of hypoechoic to hyperechoic foci or material were also detected depending on the type of ingesta of the animal. The gastric fundus had homogenous, thick, convoluted folds isoechoic to the hepatic parenchyma and a thin hypoechoic outer muscular layer (Figure 10). Gastric motility was occasionally observed. The pars pylorica was difficult to visualize and evaluate as it was a small segment between the gastric fundus and duodenum that often collapsed without ingesta.

The duodenum was located medially between the gastric fundus on the left and the fat body on the right in the mid-coelom region. It was oriented in two coiled loops within one another with the pancreas in between the limbs of the loops. The structure could be visualized in 5/7 crocodilians via the right flank and the ventral midline (Figure 3, transducer positions 7 and 14). Longitudinally, the double duodenal loops appeared as 2 curved elongated segments (Figure 11A) or 4 parallel segments with hyperechoic pancreatic lobules between them. Roughly 3 layers of the duodenum were identified including a hyperechoic empty lumen in the center, and hypoechoic inner (mucosa) and hyperechoic outer layers (submucosa and serosa). On transverse, the duodenal loops appeared as 4 circular structures arranged in a line with a hyperechoic center and outer rim with hyperechoic pancreas surrounding the middle two loops. (Figure 11B).

With the fat body occupying the right coelom, the other parts of the small intestines were mostly caudal to the stomach in the left coelom. The jejunum and ileum could not be individually distinguished. The presence of ovarian follicles in the female crocodilians also largely interfered with the visibility of the intestines. The descending colon was identified in 4/7 animals in the mid-caudal coelom dorsally when distended with hyperechoic luminal content. However the visibility of the colonic wall was obscured by its echogenicity and acoustic shadowing. The probe could be positioned either on the mid-left or right flank or ventrally.

3.3.7 Cloaca

The cloaca was identified in the caudoventral coelom in 5/7 animals when distended with anechoic to hypoechoic fluid. The individual parts of the cloaca i.e. the proctodeum, urodeum and

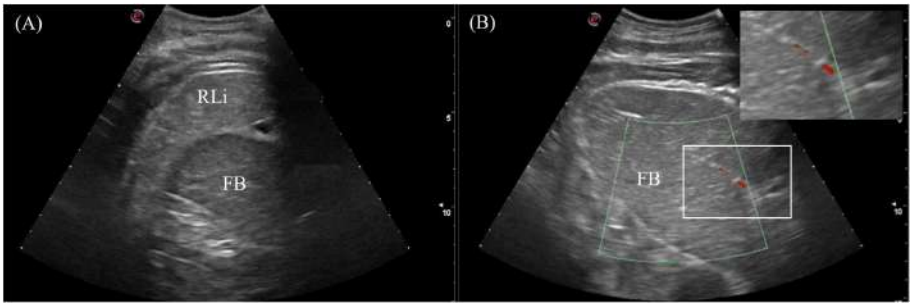

FIGURE 8
Ultrasonographic appearance of **(A)** the fat body from right lateral view and **(B)** the vascularity of the fat body using color Doppler function in *Alligator sinensis*. Note that the vasculatures are colored in red with the application of zoom function to magnify the display in the sonogram.

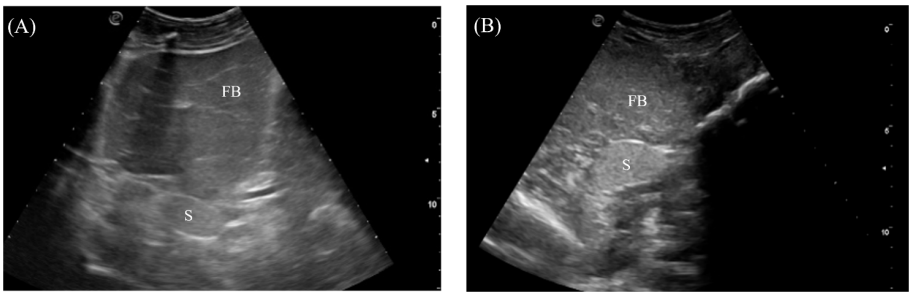

FIGURE 9
Ultrasonographic appearance of the spleen in **(A)** sagittal and **(B)** transverse views from the right lateral approach in *Alligator sinensis*. [FB, fat body; Sp, spleen].

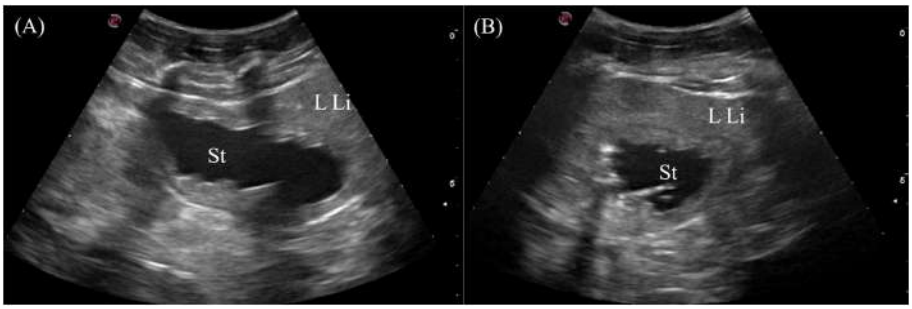

FIGURE 10
Ultrasonographic appearance of the gastric fundus in **(A)** sagittal and **(B)** transverse views from the left lateral approach in *Alligator sinensis*. [LLi, left liver lobe; St, stomach].

coprodeum might not be able to determine if the compartments were empty. The colorectum and cloaca seemed to be firmly separated by a strong sphincter since urine and feces were clearly confined in two separate compartments. From the lateral flanks, the cloaca was visualized extending into the pelvic canal. In dorsal recumbency, the pelvic portion could be seen by placing the transducer cranial to the vent (Figure 3, transducer position 15). The cloaca had a thick and smooth homogenous wall, slightly more hyperechoic than the adjacent musculature (Figure 12). When large amounts of hyperechoic sediments were present, the far cloacal wall could not be seen.

3.3.8 Kidneys

The left and right kidneys were identified 3/7 and 5/7 animals respectively. The kidneys were positioned in the caudodorsal coelom parasagitally extending into the pelvic canal (Figure 4). To visualize them, the transducer was placed dorsolaterally on the lateral flanks just cranial to the pelvic (Figure 3, transducer positions 5 and 9). In the longitudinal view, the kidney was irregularly elongated with tapered ends whereas in transverse the kidney had an irregular 'flower-like' shape (Figure 13). The kidney parenchyma was homogenous with slightly coarse echotexture and

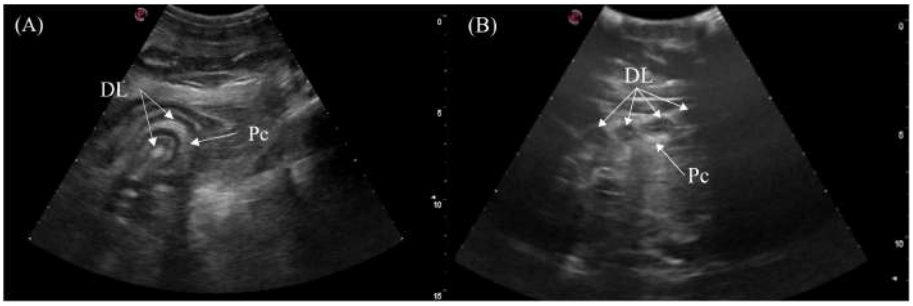

FIGURE 11
Ultrasonographic appearance of the duodenal loops in **(A)** sagittal view from the right lateral approach and **(B)** transverse view from the ventral approach in *Tomistoma schlegelii*. [DL, duodenal loops; P, pancreas].

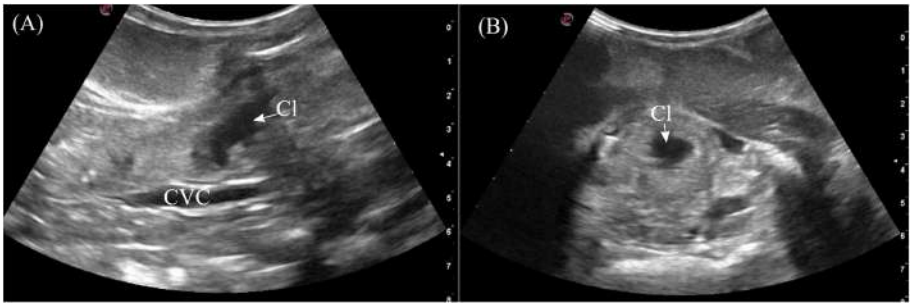

FIGURE 12
Ultrasonographic appearance of the cloaca in **(A)** sagittal and **(B)** transverse views from the ventral approach in *Alligator sinensis*. [CVC, caudal vena cava; Cl, cloaca].

isoechoic to adjacent musculature with hyperechoic rim and hilum. Vascularity was poorly detected using Doppler.

3.3.9 Gonads

The paired testes were visualized in 2/2 male crocodilians as elongated cylinders with rounded extremities cranioventral to the kidneys (Figure 3, transducer positions 4 and 8). They were homogenous and more hypoechoic than the fat body with poorly defined hyperechoic margins (Figure 14A).

In 5/5 reproductively active females, ovarian follicles were visualized in the coelomic cavity amongst the coelomic organs. The best acoustic window was via the lateral flanks just cranial to the hindlimbs and ventral to the kidneys (Figure 3, transducer position 3). The echogenicity and size of the follicles varied between and within animals depending on the stage of vitellogenesis. Most commonly seen were spherical ovarian follicles with a concentric anechoic center and hyperechoic outer rim (Figure 14B). Some ovarian follicles had an anechoic core and hypoechoic middle with a hyperechoic outline.

3.3.10 Coelomic cavity

A small to moderate amount of free anechoic fluid was detected in the male false gharial adjacent to the stomach and caudal to the fat body (Figure 15). Otherwise, no coelomic fluid was grossly detected in all other animals.

4 Discussion

This was the first study to establish a thorough ultrasonographic protocol and provide pictorial references on the normal ultrasonographic characteristics of the coelomic structures in crocodilians.

In terms of the USG protocol, the procedure itself was well-tolerated by the conscious crocodilians in this study. Although chemical sedation was not necessary throughout the entire study, the state of brumation of these crocodilians during the study period (winter season) and their familiarity with being restrained by humans may have facilitated handling. Low-frequency curvilinear probe was used to accommodate the need for higher penetration of the coelomic cavity of these large animals relative to other smaller reptiles (Holland et al., 2008; Bucy et al., 2015). Using abundant ultrasound gel was crucial in achieving sufficient surface contact for optimal imaging quality due to the nature of their rough osteoderms. The use of a stand-off pad may help improve the visualization of superficial organs although it was not used in this study (Gumpenberger, 2017). Anyhow, secure immobilization of the crocodilians itself is a crucial step before performing any physical or close-up examination on these animals. As for the probe positioning, both the left and right lateral trunks were excellent acoustic windows as there were minimal osteoderms. However, the viability of the ventrodorsal approach was affected

FIGURE 13
Ultrasonographic appearance of the right kidney in **(A)** sagittal and **(B)** transverse views and **(C)** transverse view of CT image of the kidneys in *Alligator sinensis*. [FB, fat body; LK, left kidney; RK, right kidney].

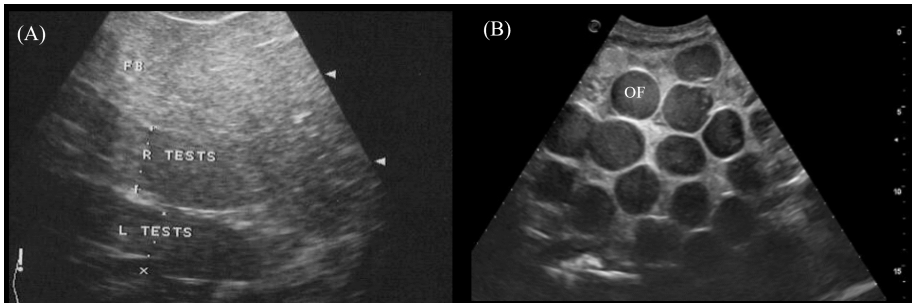

FIGURE 14
Ultrasonographic appearance of the **(A)** left and right testes in sagittal view in *Alligator sinensis* and **(B)** multiple ovarian follicles with concentric anechoic centers and hyperechoic outer rims in the coelomic cavity in *Caiman crocodilus*. [L TEST, left testis; R TEST, right testis; OF, ovarian follicles].

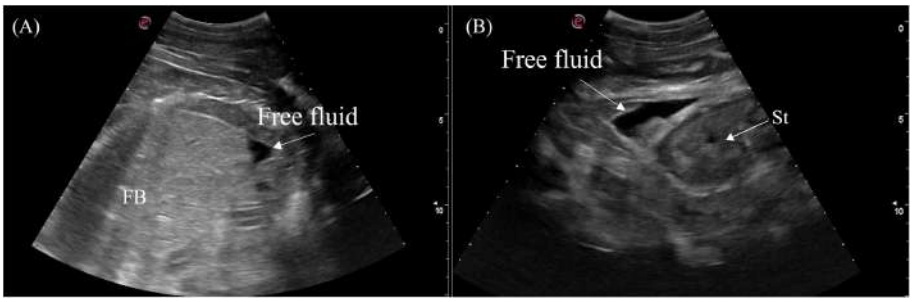

FIGURE 15
Ultrasonographic appearance of free fluid **(A)** caudal to the fat body and **(B)** adjacent to the stomach in a male *Tomistoma schlegelii*. [FB, fat body; FF, free fluid; St, stomach].

by interspecies variation in osteoderm coverage. Interference was more evident in the spectacled caiman and false gharial as their thicker ventral osteoderms impaired penetration of sound waves. Although all animals were confirmed adults based on their reproductive activity, further studies are required to investigate the changes in osteoderm coverage in relation to age in different species, which could alter the effectiveness of the ventral approach.

In regard to CT, the use of both plain and contrasted CT in conjunction with coelomic ultrasonography has allowed reliable localization of coelomic organs and evaluation of suitable acoustic windows to visualize different organs. CT eliminated superimposition artefacts seen with conventional radiography (Rademacher and Nevarez, 2019), allowing more accurate interpretation of the internal anatomy. However, the maximum CT gantry size may limit the applicability for larger crocodilians (Tsui et al., 2020). Although CT may be superior to USG in the identification of pulmonary and osseous pathological changes and even in detecting soft tissue abnormalities as acoustic shadowing could be avoided,

USG has the upper hand in terms of machine availability, portability and affordability (Kot et al., 2012; Yu et al., 2016; Vilaplana, 2019; Gumpenberger, 2021). The CT scans of the 4 different species obtained from this study would be valuable resources for further research such as describing the circulatory system and comparative anatomy e.g. the cranium and fat body morphology. The fusion imaging technique used in this study significantly improved the confidence in organ localization and correlation between CT and USG modalities. However, the downside of this technique was that any slight movement of the subject would cause discrepancies in the CT and real-time USG viewed on the display. This would lead to a need for re-synchronization thus increasing examination time. Sedation would help avoid movements, especially in active, aggressive, and nervous crocodilians.

The heart, liver, fat body, stomach, and spleen were clearly visualized because of their size, fixed location and distinctive appearances. Thorough evaluation of the heart and liver lobes would require the incorporation of probe movement along the respiratory cycle as these organs are located within the thoracic space. There is also a lack of reference literature that describes the gross anatomy of hepatic vasculature in crocodilians although it appears to be similar to reptiles (Yeager, 1973). Hepatic veins could be identified by tracing from the caudal vena cava. The gallbladder, colon and cloaca were visualized when distended with luminal content. The visibility of the luminal wall of the gastric fundus, colon and cloaca was mainly obstructed when luminal hyperechoic debris cast acoustic shadowing onto the far wall. The ultrasonographic description of the gastric fundus was determined with reference to histological descriptions of previous studies as histology was not performed in this study (Shaker and Ibrahium, 2020; Takasaki and Kobayashi, 2020). Visualization of the kidneys and testes of the crocodilians was subjective to the observer's experience due to their irregularity and similar ultrasonographic appearance with adjacent musculature. The pancreas was a poorly discernible organ in this study and was identified as hyperechoic tissue interspersed in between the duodenal loops. The ultrasonographic appearance of the ovarian follicles has been described in the American alligators (*Alligator mississippiensis*) by Lance et al. (2009). and was similar to the 4 species included in this study.

In the clinical context, USG would be a valuable tool for health evaluation and disease diagnosis in crocodilians. For instance, intracelomic diseases such as hepatitis can be identified (Martelli, 2019) and ultrasound-guided biopsy may be performed as indicated in other reptilian species (Divers and Cooper, 2000). Other diseases such as splenic, pancreatic or renal diseases, masses and reproductive disorders could also be identified via USG (Holland et al., 2008). Although the intestinal tract was poorly visualized in these 'healthy' crocodilians, visibility may improve with pathological processes causing structural changes in the intestinal tract. Additionally, the current method of assessing the nutritional status in crocodilians has been based on the fat body:heart weight ratio in dissected animals (Huchzermeyer, 2003). The feasibility of using USG to examine the fat body and heart suggests a possibility of evaluating the nutritional status of live crocodilians by comparing their longitudinal and transverse dimensions, though further research is needed. The ability of 3D volume rendering with the CT images would also be useful for the same purpose (Kot et al., 2018, 2020a, 2020b, 2022a, 2022b, 2024).

There were several limitations to this study. Quantitative observations were not recorded because of a small sample size, and the use of 4 different species precluded valid statistical analysis. The physiological dynamic nature of some organs such as the fat body, gallbladder, and kidneys also complicated the measurement of organ dimensions. Moreover, because the fat body was more hyperechoic than the liver only in the spectacled caiman and free coelomic fluid was only determined in one false gharial, these findings could be either pathological or physiological. The amount of coelomic fluid considered normal or pathological is indeed not determinable yet, due to a lack of literature indicating the normal reference range. Including a larger sample size with a more heterogenous population of crocodilians of similar species with different age groups and sizes would help describe the normal appearances of coelomic organs more accurately. Although the cardiac structures were visible in this study, a detailed dynamic echocardiography was difficult to obtain. Another study has described the use of transesophageal echocardiographic technique in assessing the complex cardiac anatomy hemodynamics in Nile crocodiles (Poulsen et al., 2024)

In conclusion, USG could be safely performed on conscious crocodilians with appropriate restraint and should be considered as part of health assessment protocols of crocodilians, especially those in captivity, either for tourism, conservation or farming purposes. A standardized imaging protocol will contribute to a systematic approach to assessing the health of crocodilians, reducing animal handling time and increasing the validity of imaging examinations. The findings of this study will facilitate the interpretation and diagnosis of intracoelomic abnormalities via ultrasound by providing a reference of normal appearances of coelomic organs. In terms of conservation, the imaging protocol will be beneficial as part of population health assessments of wild or captive endangered species and pre-release health assessments to identify potential pathologies. It will be a valuable guide for field researchers, crocodile farm staff, veterinarians, and aquarium staff to improve disease diagnosis and thereby apply more precise therapy.

Data availability statement

The original contributions presented in the study are included in the article/supplementary material. Further inquiries can be directed to the corresponding author.

Ethics statement

The animal study was approved by Animal Research Ethics Sub-Committee, City University of Hong Kong, 3 conservation institutes and Animals (Control of Experiments) Ordinance (Cap. 340) from the Department of Health, Hong Kong. The study was conducted in accordance with the local legislation and institutional

requirements. Written informed consent was obtained from the individual(s) for the publication of any identifiable images or data included in this article.

Author contributions

WY: Writing – review & editing, Writing – original draft, Investigation, Formal analysis, Data curation, Conceptualization. PM: Writing – review & editing, Visualization, Validation, Supervision, Methodology, Investigation, Data curation, Conceptualization. TC: Writing – review & editing, Visualization, Validation, Supervision, Methodology, Data curation. HT: Data curation, Writing – review & editing, Visualization, Validation, Supervision, Methodology. TG: Writing – review & editing, Visualization, Validation, Supervision, Methodology, Data curation. BK: Writing – review & editing, Visualization, Validation, Supervision, Project administration, Methodology, Investigation, Funding acquisition, Formal analysis, Data curation, Conceptualization.

Funding

The author(s) declare financial support was received for the research, authorship, and/or publication of this article. This project is financially funded by the course VM4401 Research Project in the Bachelor of Veterinary Medicine, Jockey Club College of Veterinary Medicine and Life Sciences, City University of Hong Kong; and Research Matching Grant Scheme (No. 9229157, 9229186) of University Grants Committee of the Hong Kong Special Administrative Region, China.

Acknowledgments

We would like to thank the Agriculture, Fisheries and Conservation Department of the Hong Kong Special Administrative Region Government, the veterinary and husbandry teams from Ocean Park Hong Kong, Dr. Alex Grioni, Dr. Renata Snow, Ms. Debbie Ng from Kadoorie Farm and Botanical Garden, and the team from Hong Kong Wetland Park for allowing the crocodilians under their care to be included in the study. Sincere appreciation is also extended to Ocean Park Hong Kong for providing the location and CT unit, as well as Chavon Medical Systems Limited for providing the USG unit, logistic support and technical assistance to conduct the study.

Conflict of interest

The authors declare that the research was conducted in the absence of any commercial or financial relationships that could be construed as a potential conflict of interest.

Publisher's note

References

Brazaitis, P., and Watkins-Colwell, G. (2011). A brief history of crocodilian science. *Herpetol. Rev.* 42, 483–496.

Bucy, D. S., Guzman, D. S.-M., and Zwingenberger, A. L. (2015). Ultrasonographic anatomy of bearded dragons (*Pogona vitticeps*). *J. Am. Vet. Med. Assoc.* 246, 868–876. doi: 10.2460/javma.246.8.868

Divers, S. J., and Cooper, J. E. (2000). Reptile hepatic lipidosis. *J. Exot. Pet Med.* 9, 153–164. doi: 10.1053/ax.2000.7136

Gumpenberger, M. (2017). Diagnostic imaging of reproductive tract disorders in reptiles. *Vet. Clin. North Am. Exot. Anim. Pract.* 20, 327–343. doi: 10.1016/j.cvex.2016.11.003

Gumpenberger, M. (2021). Diagnostic imaging of the respiratory tract of the reptile patient. *Vet. Clin. North Am. Exot. Anim. Pract.* 24, 293–320. doi: 10.1016/j.cvex.2021.01.002

Holland, M. F., Hernandez-Divers, S., and Frank, P. M. (2008). Ultrasonographic appearance of the coelomic cavity in healthy green iguanas. *J. Am. Vet. Med. Assoc.* 233, 590–596. doi: 10.2460/javma.233.4.590

Huchzermeyer, F. W. (2003). Crocodiles – Biology, husbandry and diseases. *J. S Afr. Vet. Assoc.* 74 (4), a529. doi: 10.1079/9780851996561.0000

IUCN Crocodile Specialist Group (2022a). *Classification of Living Crocodilians*. Available online at: http://www.iucncsg.org/pages/Classification-of-Living-Crocodilians.html (Accessed November 18, 2022).

IUCN Crocodile Specialist Group (2022b). *Crocodilian Capacity Building Manual*. Available online at: http://www.iucncsg.org/pages/Crocodilian-Capacity-Building-Manual-.html (Accessed September 28, 2022).

Kot, B. C. W., Chan, D. K. P., Chung, T. Y. T., and Tsui, H. C. L. (2020a). Image rendering techniques in postmortem computed tomography: evaluation of biological health and profile in stranded cetaceans. *JoVE* 163, e61701. doi: 10.3791/61701

Kot, B. C. W., Chan, D. K. P., Yuen, A. H. L., and Tsui, H. C. L. (2018). Diagnosis of atlanto-occipital dissociation: Standardised measurements of normal craniocervical relationship in finless porpoises (genus *Neophocaena*) using postmortem computed tomography. *Sci. Rep.* 8, 8474. doi: 10.1038/s41598-018-26866-8

Kot, B. C. W., Fernando, N., Gendron, S., Heng, H. G., and Martelli, P. (2016). "The virtopsy approach: bridging necroscopic and radiological data for death investigation of stranded cetaceans in the Hong Kong waters," in *IAAAM 47th Annual Conference Proceedings* (IAAAM, Virginia Beach, VA).

Kot, B. C. W., Ho, H. H. N., Leung, E. K. C., Chung, T. Y. T., and Tsui, H. C. L. (2022a). Characterisation of *Crassicauda fuelleborni* nematode infection in Indo-Pacific finless porpoises (*Neophocaena phocaenoides*) using postmortem computed tomography. *IJP-PAW* 18, 68–75. doi: 10.1016/j.ijppaw.2022.04.005

Kot, B. C. W., Ho, H. H. N., Martelli, P., Churgin, S. M., Fernando, N., Lee, F. K., et al. (2022b). An Indo-Pacific humpback dolphin (*Sousa chinensis*) severely injured by vessel collision: live rescue at sea, clinical care, and postmortem examination using a virtopsy-integrated approach. *BMC Vet. Res.* 18, 417. doi: 10.1186/s12917-022-03511-1

Kot, B. C., Sin, D. M., and Ying, M. (2009). Evaluation of the accuracy and reliability of two 3-dimensional sonography methods in volume measurement of small structures: an *in vitro* phantom study. *J. Clin. Ultrasound* 37, 82–88. doi: 10.1002/jcu.20525

Kot, B. C. W., Tsui, H. C. L., Chung, T. Y. T., and Lau, A. P. Y. (2020b). Postmortem neuroimaging of cetacean brains using computed tomography and magnetic resonance imaging. *Front. Mar. Sci.* 7. doi: 10.3389/fmars.2020.544037

Kot, B. C. W., Yeong, J. W. Y., Kwan, A. S. Y., Ho, G. Y. H., Ho, H. H. N., Tsui, H. C. L., et al. (2024). Illustrated cross-sectional computed tomography of the cetacean abdomino-pelvic organs. *Ann. Anat* 256, 152317. doi: 10.1016/j.aanat.2024.152317

Kot, B. C., Ying, M. T., Brook, F. M., Kinoshita, R. E., and Cheng, S. C. (2012). Ultrasonographic assessment of the thyroid gland and adjacent anatomic structures in Indo-Pacific bottlenose dolphins (*Tursiops aduncus*). *Am. J. Vet. Res.* 73, 1696–1706. doi: 10.2460/ajvr.73.11.1696

Lance, V. A., Rostal, D. C., Elsey, R. M., and Trosclair, P. L. (2009). Ultrasonography of reproductive structures and hormonal correlates of follicular development in female American alligators, *Alligator mississippiensis*, in southwest Louisiana. *Gen. Comp. Endocrinol.* 162, 251–256. doi: 10.1016/j.ygcen.2009.03.021

Latip, M. Q. A., Tengku Azizan, T. R. P., Ahmad, H., Abu Hassim, H., Noor, M. H. M., and Mikail, M. (2021). Blood profiling of captive and semi-wild false gharial in peninsular Malaysia. *Anim. (Basel)* 11, 1481. doi: 10.3390/ani11061481

Lovely, C. J., Pittman, J. M., and Leslie, A. J. (2007). Normal haematology and blood biochemistry of wild Nile crocodiles (*Crocodylus niloticus*) in the Okavango Delta, Botswana. *J. S Afr. Vet. Assoc.* 78, 137–144. doi: 10.4102/jsava.v78i3.305

Martelli, P. R. (2019). "59 - Medical Evaluation of Crocodilians," in *Fowler's Zoo and Wild Animal Medicine Current Therapy*, vol. 9 . Eds. R. E. Miller, N. Lamberski and P. P. Calle (W.B. Saunders, St. Louis (MO). doi: 10.1016/B978-0-323-55228-8.00059-X

McDougald, W., Vanhove, C., Lehnert, A., Lewellen, B., Wright, J., Mingarelli, M., et al. (2020). Standardization of preclinical PET/CT imaging to improve quantitative accuracy, precision, and reproducibility: A multicenter study. *J. Nucl. Med.* 61, 461–468. doi: 10.2967/jnumed.119.231308

Nevarez, J. (2019). "136 — Differential Diagnosis by Clinical Signs - Crocodilians," in *Mader's Reptile and Amphibian Medicine and Surgery, 3rd ed*. Eds. S. J. Divers and S. J. Stahl (W.B. Saunders, St. Louis (MO). doi: 10.1016/B978-0-323-48253-0.00136-7

Nifong, J. (2018). *6.4. Ecological value of crocodilians. Crocodilian Capacity Building Manual*. Available online at: http://www.iucncsg.org/pages/Crocodilian-Capacity-Building-Manual-.html (Assessed October 22, 2022).

Pang, B. S., Kot, B. C., and Ying, M. (2006). Three-dimensional ultrasound volumetric measurements: is the largest number of image planes necessary for outlining the region-of-interest? *Ultrasound Med. Biol.* 32, 1193–1202. doi: 10.1016/j.ultrasmedbio.2006.04.012

Peng, F., Chen, X., Meng, T., Li, E., Zhou, Y., and Zhang, S. (2018). Hematology and serum biochemistry parameters of captive Chinese alligators (*Alligator sinensis*) during the active and hibernating periods. *Tissue Cell.* 51, 8–13. doi: 10.1016/j.tice.2018.02.002

Poulsen, C. F. B., Munk, K., Wang, T., and Damkjaer, M. (2024). Transesophageal echocardiography of cardiac function in Nile crocodiles – A novel tool for assessing complex hemodynamic patterns. *Comparative Biochemistry and Physiology Part A: Molecular & Integrative Physiology* 288, 111564. doi: 10.1016/j.cbpa.2023.111564

Rademacher, N., and Nevarez, J. G. (2019). "57 - Radiography—Crocodilians," in *Mader's Reptile and Amphibian Medicine and Surgery, 3rd ed*. Eds. S. J. Divers and S. J. Stahl (W.B. Saunders, St. Louis (MO)).

Ross, J. P. (1998). *Crocodiles: status survey and conservation action plan* (UK: IUCN/SCC Crocodile Specialist Group. IUCN, Gland, Switzerland and Cambridge).

Shaker, N., and Ibrahium, D. (2020). Anatomical and Histological Features of the Gastrointestinal Tract in the Nile Crocodile, (*Crocodylus Niloticus*) with Special reference to its Arterial Blood Supply. *Adv. Anim. Vet. Sci.* 9, 692-699. doi: 10.17582/journal.aavs/2021/9.5.692.699

Takasaki, R., and Kobayashi, Y. (2020). Stomach histology of *Crocodylus siamensis* and *Gavialis gangeticus* reveals analogy of archosaur "gizzards", with implication on crocodylian gastroliths function. *Acta Herpetol.* 15 (2), 111–118. doi: 10.13128/a_h-7564

Tsui, H. C. L., Kot, B. C. W., Chung, T. Y. T., and Chan, D. K. P. (2020). Virtopsy as a revolutionary tool for cetacean stranding programs: implementation and management. *Front. Mar. Sci.* 7. doi: 10.3389/fmars.2020.542015

Tucker, A., and Limpus, C. (1997). Assessment of reproductive status in Australian freshwater crocodiles (*Crocodylus johnstoni*) by ultrasound imaging. *Copeia* 1997 (4), 851–857. doi: 10.2307/1447305

Van Der Merwe, N. J., and Kotze, S. H. (1993). The topography of the thoracic and abdominal organs of the Nile crocodile (*Crocodylus niloticus*). *Onderstepoort J. Vet. Res.* 60, 219–222.

Vilaplana, G. F. (2019). Orthopedic diagnostic imaging in exotic pets. *Vet. Clin. North Am. Exot. Anim. Pract.* 22, 149–173. doi: 10.1016/j.cvex.2019.01.003

Yeager, V. L. (1973). The vascular anatomy of the liver of the monitor lizard (genus varanus). *Am. J. Anat.* 136, 441–453. doi: 10.1002/aja.1001360405

Yu, X., Hao, Y., Kot, B. C. W., and Wang, D. (2016). Effect of photoperiod extension on the testicular sonographic appearance and sexual behavior of captive Yangtze finless porpoise (*Neophocaena asiaeorientalis asiaeorientalis*). *Zool. Stud.* 55, e24. doi: 10.6620/ZS.2016.55-24